JOURNAL OF MATERIALS SCIENCE 39 (2004) 6523–6528

Dielectric dispersion and tunability of sol-gel derived $Ba_xSr_{1-x}TiO_3$ thin films

S. U. ADIKARY*
Department of Applied Physics and Materials Research Centre, The Hong Kong Polytechnic University, Hung Hom, Kowloon, Hong Kong; Department of Materials Engineering, University of Moratuwa, Moratuwa, Sri Lanka
E-mail: suadikary@yahoo.com

H. L. W. CHAN
Department of Applied Physics and Materials Research Centre, The Hong Kong Polytechnic University, Hung Hom, Kowloon, Hong Kong

$Ba_{0.5}Sr_{0.5}TiO_3$, $Ba_{0.6}Sr_{0.4}TiO_3$, $Ba_{0.7}Sr_{0.3}TiO_3$ and $Ba_{0.8}Sr_{0.2}TiO_3$ thin films were fabricated by a modified sol-gel technique on Pt(111)/Ti/SiO_2/Si(100) substrates. All $Ba_xSr_{1-x}TiO_3$ films crystallized in the perovskite structure with a crack free microstructure and clear grain boundaries. Highest relative permittivity and dielectric tunability was observed in the $Ba_{0.7}Sr_{0.3}TiO_3$ thin film. $Ba_{0.7}Sr_{0.3}TiO_3$ and $Ba_{0.8}Sr_{0.2}TiO_3$ compositions demonstrated ferroelectric hysteresis loops indicating the presence of ferroelectricity at room temperature. The paraelectric compositions of $Ba_{0.5}Sr_{0.5}TiO_3$ and $Ba_{0.6}Sr_{0.4}TiO_3$ showed significant tunability with negligible loss tangent. The tunability of $Ba_{0.5}Sr_{0.5}TiO_3$ thin film decreased with the increase of frequency from 100 kHz to 100 MHz. As the frequency increases, especially above 10 MHz, the relative permittivity decreases while the loss tangent increases. Since $Ba_{0.5}Sr_{0.5}TiO_3$ thin film is paraelectric at room temperature, relaxation due to ferroelectric domains cannot occur. Therefore this behaviour has originated from the contact resistance and finite sheet resistance of both the bottom and top electrodes. To analyse the thin film capacitor, the parallel plate capacitor structure can be modeled based on an equivalent circuit, which contain electrode and contact resistance.

1. Introduction

The $Ba_xSr_{1-x}TiO_3$ (BST) system is of considerable interest to researchers and engineers in the field of electroceramics and microelectronics [1, 2]. Barium strontium titanate (BST) can be considered as a solid solution of strontium titanate and barium titanate. $SrTiO_3$ shows a perovskite cubic structure while $BaTiO_3$ exhibits a perovskite tetragonal structure at room temperature. The Curie temperature of $Ba_xSr_{1-x}TiO_3$ system decreases linearly with the increasing amounts of Sr in the $BaTiO_3$ lattice. This enables the ferroelectric/paraelectric transition temperature to be tailored for specific applications by varying the Sr content. In general, at room temperature, $Ba_xSr_{1-x}TiO_3$ is ferroelectric when $x > 0.7$ and paraelectric when $x < 0.7$ [2]. The research interest in BST thin films has originated from its potential applications in integrated devices and the possible advantages of low operating voltages and high switching speeds [3]. Therefore, BST thin films are good candidates for applications in dynamic random access memories (DRAM), IR detectors, capacitor-varistor protection devices, etc. [4–6]. BST thin films are attractive to many of these applications mainly due to its high dielectric permittivity and low loss tangent. Recent research interest in high frequency and microwave materials has shown good potential for BST materials to be used in high frequency applications as resonators, tunable devices, filters, wave guides etc. [7, 8]. The thin film form of BST is a potential candidate for active microwave tunable devices because of its variable relative permittivity under an external electric field.

Among the various techniques available for thin film fabrication, the sol-gel method offers a simple way of controlling the composition and achieving high homogeneity. The low capital cost of the equipment and simplicity make it an excellent technique for trials of new compositions and modifying conventional fabrication techniques. Also, in thin film fabrication, the sol-gel process can be used for large and complex area deposition.

In this work, $Ba_{0.5}Sr_{0.5}TiO_3$, $Ba_{0.6}Sr_{0.4}TiO_3$, $Ba_{0.7}Sr_{0.3}TiO_3$ and $Ba_{0.8}Sr_{0.2}TiO_3$ thin films were fabricated by a modified sol-gel method on a Pt/Ti/SiO_2/Si substrate. Ferroelectric and dielectric behaviour of

* Author to whom all correspondence should be addressed.

BST thin films were analysed as a function of film composition. High frequency dielectric tunability of BST thin films with room temperature paraelectric and ferroelectric compositions are presented and discussed. The effects of contact resistance and finite sheet resistance of electrode materials on the high frequency dielectric properties are discussed.

2. Experimental procedure

The multicomponent $Ba_xSr_{1-x}TiO_3$ precursor solution was synthesized using barium acetate [$Ba(CH_3CO_2)_2$, *Acros*], strontium acetate [$Sr(CH_3CO_2)_2$, *Strem*] and titanium (iv)*n*-butoxide [$Ti(O(CH)_3CH_3)_4$, *Acros*] as starting materials. Acetic acid [CH_3COOH] was used as the basic solvent. At first, stoichiometric weights of barium acetate and strontium acetate were mixed in acetic acid. During the mixing, solution was heated to about 100°C and the mixing was continued until all the starting materials were dissolved. Stoichiometric weight of Ti(iv)*n*-butoxide was first dissolved in 2-methoxyethanol to prevent hydrolysis of the butoxide. Then the Ti(iv)*n*-butoxide solution was mixed with the solution containing barium and strontium components. The mixing was continued until a clear solution was obtained. Then ethylene glycol was added as a chelating agent to control the hydrolysis rates of the highly reactive alkoxides. After the preparation of a stable solution, it was aged for about 24 h. before the film fabrication.

Highly diluted precursor solutions of 0.05 M concentrations were spin coated on $Pt/Ti/SiO_2/Si$ substrates. Then the film was subjected to a controlled heat treatment cycle in a rapid thermal processor. At first, the film was heated to 120°C for 120 s and then the temperature was increased to 400°C for 120 s. Finally the temperature was raised to 750°C and annealed for 120 s in oxygen atmosphere. After spin coating of each layer, the heat treatment cycle was repeated. The spin coating and heat treatment cycles were repeated to achieve the desired thickness. Finally, the bulk film was annealed at 750°C in oxygen atmosphere for 10 min. A detailed account on sample preparation is given elsewhere [9].

The phase formation and the crystallisation were analysed using a Philips PW3710 X-ray diffractometer (XRD) in a glancing angle mode with Cu K_α radiation. The surface morphology and the grain structure were investigated using a Leica stereo scan 440 scanning electron microscope (SEM). Rutherford backscattering spectroscopy was used to analyse the chemical composition of BST thin films. To study the dielectric and ferroelectric properties, 0.2 mm diameter Au/Cr circular electrodes were sputtered through a shadow mask to form a metal-ferroelectric-metal (MFM) configuration. The bottom Pt electrode was exposed by etching a small portion of the film using dilute hydrofluoric acid. Cross-sectional SEM micrographs were used to determine the film thickness. The thickness values determined from the cross sectional SEM micrographs were $Ba_{0.8}Sr_{0.2}TiO_3$ ~290 nm, $Ba_{0.7}Sr_{0.3}TiO_3$ ~280 nm, $Ba_{0.6}Sr_{0.4}TiO_3$ ~250 nm, and $Ba_{0.5}Sr_{0.5}TiO_3$ ~240 nm.

The low frequency (100 Hz–1 MHz) dielectric properties of BST films were measured using an Agilent 4294A impedance/gain phase analyzer with an Agilent 42941A impedance probe. Measurements in the RF (radio frequency) region were done using an HP 4291B RF impedance analyzer with Cascade microprobes. Built-in DC bias system of the impedance analyzer was used to apply the electric field. Before the measurements, the system was calibrated for short, open and load. Polarization-electric field (P-E) hysteresis loop measurements were carried out using a modified Sawyer-Tower circuit at a frequency of 100 Hz.

3. Results and discussion

The glancing incidence X-ray diffraction patterns of $Ba_{0.5}Sr_{0.5}TiO_3$, $Ba_{0.6}Sr_{0.4}TiO_3$, $Ba_{0.7}Sr_{0.3}TiO_3$ and $Ba_{0.8}Sr_{0.2}TiO_3$ thin films are shown in Fig. 1. The glancing angle mode was used to avoid the disturbance from the strong Pt (111) diffraction peak of the bottom electrode. It is seen that the $Ba_xSr_{1-x}TiO_3$ films are polycrystalline and contain only characteristic BST and Pt peaks [10, 11]. Spurious phases were not observed. Therefore the perovskite phase formation of the $Ba_xSr_{1-x}TiO_3$ thin films is confirmed by the X-ray diffraction patterns. According to the XRD patterns, the strong Pt (220) peak from the bottom electrode overlap with the BST (220) peak. However Pt (111) peak does not have any significant influence on the XRD patterns. As the Sr content of the $Ba_xSr_{1-x}TiO_3$ increased, the diffraction lines shifted towards the larger angles. This indicates the decrease in lattice spacing with the increase in Sr content in the $Ba_xSr_{1-x}TiO_3$ lattice. The difference in size between the Ba^{2+}ion ($r = 0.135$ nm) and the Sr^{2+} ion ($r = 0.113$ nm) contributes to this behaviour. Since both $BaTiO_3$ and $SrTiO_3$ crystallize to the same perovskite structure, the

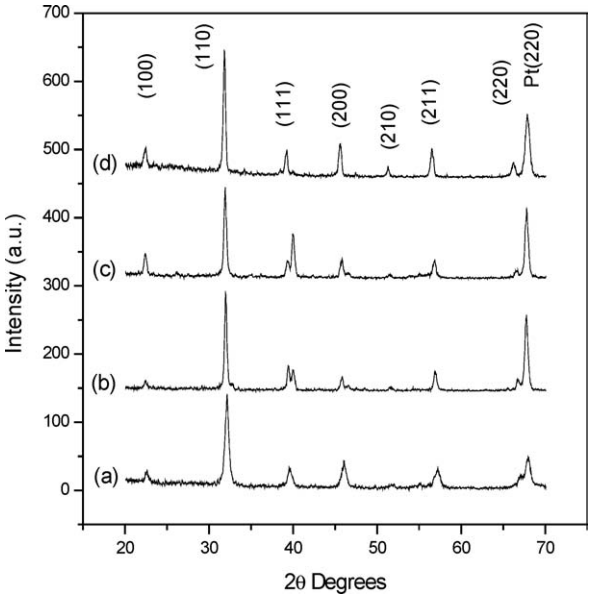

Figure 1 Glancing incidence X-ray diffraction patterns of sol-gel derived $Ba_xSr_{1-x}TiO_3$ thin films on $Pt/Ti/SiO_2/Si$ substrates: (a) $Ba_{0.5}Sr_{0.5}TiO_3$, (b) $Ba_{0.6}Sr_{0.4}TiO_3$, (c) $Ba_{0.7}Sr_{0.3}TiO_3$, and (d) $Ba_{0.8}Sr_{0.2}TiO_3$.

TABLE I Relative permittivity, loss tangent and dielectric tunability of $Ba_xSr_{1-x}TiO_3$ thin films measured at 100 kHz and 10 MHz

Film composition (Ba/Sr)	0.5/0.5	0.6/0.4	0.7/0.3	0.8/0.2
Relative permittivity				
100 kHz	589.7	607.8	778.3	638.1
10 MHz	536.7	540.1	668.8	523.2
Loss tangent				
100 kHz	0.01	0.03	0.04	0.02
10 MHz	0.08	0.09	0.11	0.13
Tunability (%)				
100 kHz	35.6	36.1	41.7	35.8
10 MHz	33.9	34.3	39.1	30.1

size difference of Ba and Sr ions is reflected in the lattice parameters.

Relative permittivity (ε_r), loss tangent ($\tan\delta$) and dielectric tunability data of BST thin films are given in Table I. Generally, with the application of DC electric field, the dielectric tunability is defined as $[\varepsilon_r(\max) - \varepsilon_r(\min)]/\varepsilon_r(\max)$ [12]. The relative permittivity of BST thin films increases with the increase of Ba content up to $Ba_{0.7}Sr_{0.3}TiO_3$ composition and then starts to decrease. The dielectric tunability shows the same tendency with the increasing Ba composition as in the case of relative permittivity. This can be explained by considering the locations of the Curie temperature (T_c) of various $Ba_xSr_{1-x}TiO_3$ compositions [11, 13]. Tunability in the paraelectric phase is attractive due to the low dielectric losses at higher frequencies. The magnitude of the dielectric tunability depends on the of applied field and the electrode configuration [14]. Dielectric tunabilities of $Ba_{0.5}Sr_{0.5}TiO_3$and $Ba_{0.7}Sr_{0.3}TiO_3$thin films are shown in Fig. 2a and b respectively. Highest relative permittivity and dielectric tunability was observed in $Ba_{0.7}Sr_{0.3}TiO_3$ thin films. The T_c of $Ba_{0.7}Sr_{0.3}TiO_3$ is around room temperature thereby giving very high relative permittivity values at room temperature. But compositions like $Ba_{0.5}Sr_{0.5}TiO_3$ show lower permittivity due to wide difference between room temperature and T_c. $Ba_{0.8}Sr_{0.2}TiO_3$ and $Ba_{0.7}Sr_{0.3}TiO_3$ thin films showed observable polarization-electric field (P-E) hysteresis loops as shown in Fig. 3. This observation indicates the presence of ferroelectricity in $Ba_{0.8}Sr_{0.2}TiO_3$ and $Ba_{0.7}Sr_{0.3}TiO_3$ compositions. In general, the dielectric losses are usually higher in the ferroelectric materials at higher frequencies due to the ferroelectric relaxation [15]. Thin films of $Ba_{0.5}Sr_{0.5}TiO_3$ and $Ba_{0.6}Sr_{0.4}TiO_3$ compositions are paraelectric at room temperature and therefore more suitable for high frequency applications. The dielectric tunabilities of $Ba_{0.5}Sr_{0.5}TiO_3$ and $Ba_{0.6}Sr_{0.4}TiO_3$ films are quite good for our thin films considering the polycrystalline nature and $Pt/Ti/SiO_2/Si$ substrates [12]. $Ba_{0.6}Sr_{0.4}TiO_3$ composition shows higher tunability because of its close proximity to the Curie temperature. From Table I, it can be seen that even at a high frequency of 10 MHz, the relative permittivity values of paraelectric compositions are higher and the loss tangent is comparatively lower. However, the continuous increase in frequency tends to gradually decrease the relative permittivity and increase the loss tangent. This inevitably results in lower dielectric tunability. It can be seen from Fig. 4 that the tunability has decreased at 100 MHz compared to that at 100 kHz for the $Ba_{0.5}Sr_{0.5}TiO_3$ thin film. At frequencies lower than 1 MHz, the tunability is more or less constant and with the increase of frequency above 1 MHz, a decrease in the tunability can be observed. In general, tunability is roughly proportional to the relative permittivity. Usually, a material with higher relative permittivity possesses larger tunability [13]. Therefore, the behaviour of tunability as a function of frequency can be investigated by studying the dielectric dispersion with frequency.

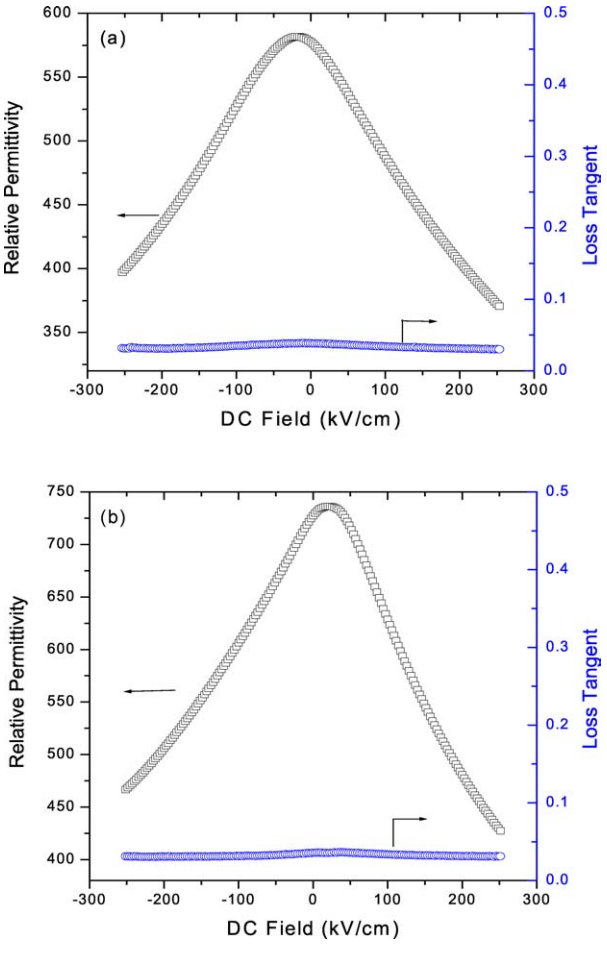

Figure 2 Relative permittivity as a function of DC electric field of $Ba_xSr_{1-x}TiO_3$ thin films at 100 kHz: (a) $Ba_{0.5}Sr_{0.5}TiO_3$ and (b) $Ba_{0.7}Sr_{0.3}TiO_3$.

The relative permittivity and loss tangent of $Ba_{0.5}Sr_{0.5}TiO_3$ and $Ba_{0.7}Sr_{0.3}TiO_3$ thin films as a function of frequency was measured from 100 Hz to 100 MHz and given in Fig. 5. In $Ba_{0.5}Sr_{0.5}TiO_3$ thin film, a slight decrease in relative permittivity can be observed in the whole frequency region. But in $Ba_{0.7}Sr_{0.3}TiO_3$ thin film a significant dielectric dispersion can be observed. The loss tangent is almost constant up to 10 MHz for both films. But above 10 MHz a rapid increase in the loss tangent can be observed in $Ba_{0.7}Sr_{0.3}TiO_3$ film than that of $Ba_{0.5}Sr_{0.5}TiO_3$ film. Since $Ba_{0.7}Sr_{0.3}TiO_3$ film showed ferroelectric properties at room temperature, the dispersion in the MHz range is due to the relaxation of ferroelectric domain walls. However, $Ba_{0.5}Sr_{0.5}TiO_3$ film is paraelectric at

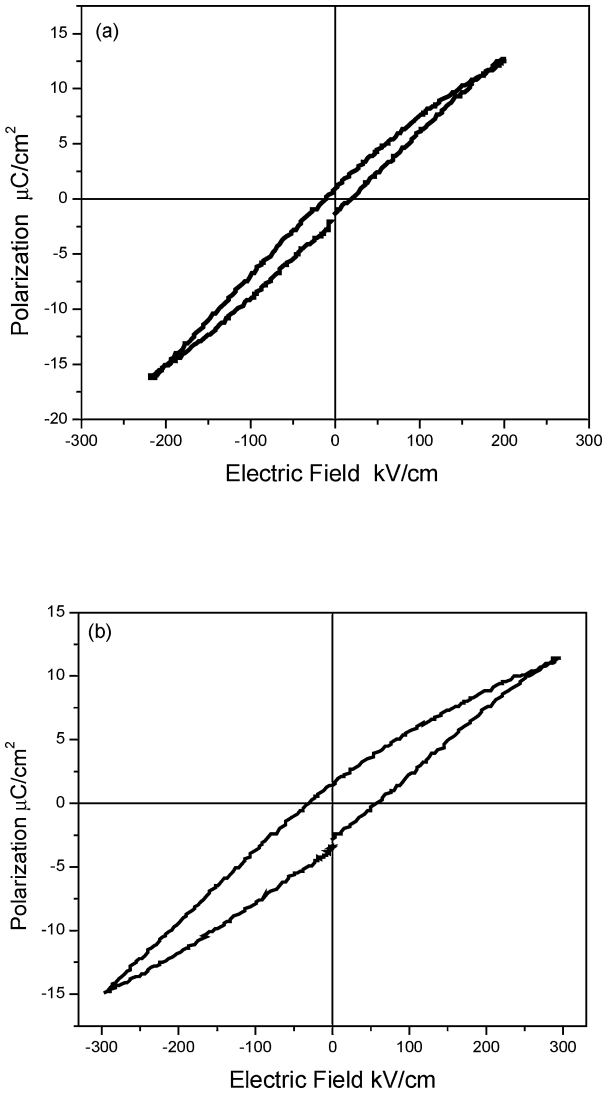

Figure 3 Polarization-electric field (P-E) hysteresis loops for $Ba_xSr_{1-x}TiO_3$ thin films at room temperature: (a) $Ba_{0.7}Sr_{0.3}TiO_3$ and (b) $Ba_{0.8}Sr_{0.2}TiO_3$.

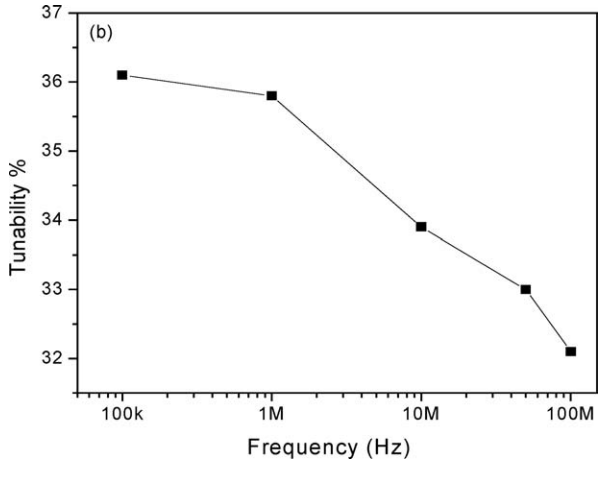

Figure 4 Dielectric tunability as a function of frequency for $Ba_{0.5}Sr_{0.5}TiO_3$ thin films under a DC field of 250 kV/cm.

room temperature and do not possess any ferroelectric properties [16]. Therefore, spontaneous polarization cannot be generated as there are no ferroelectric domains in these materials. Since there are no domain walls in these films, a ferroelectric dispersion cannot occur. But for $Ba_{0.5}Sr_{0.5}TiO_3$ film a slight decrease in relative permittivity and increase in loss tangent at higher frequencies can be observed. In recent years, many researchers working on thin films have observed high losses in the RF (radio frequency) and microwave frequencies [17]. Considerable effort has been spent to understand the dominant loss mechanisms at higher frequencies [18].

It is well known that the dielectric response from a ferroelectric thin film capacitor depends on lead inductance and electrode resistance. However, it has been shown that the contribution of capacitor loss from the resistance of metallization can predominate in the RF and microwave frequency regime [19]. The losses originate from the contact resistance and the finite sheet resistance of both the bottom and top electrodes may be present in the measured dielectric loss data [20]. The parallel plate capacitor structure of thin films can be modelled based on the equivalent circuit given in Fig. 6. For our BST thin film capacitors, high frequency losses can be ascribed to two sources of loss, namely the BST dielectric loss and the electrode loss. In Fig. 6, C_d and R_d represent the true capacitance and resistance of the dielectric film. R_s is the parasitic resistance due to the electrodes and contacts. Analysis of the model is simplified if $\tan\delta_d = 1/(\omega R_d C_d)$ for the film is small (<0.1). By neglecting the inductance effect, it can then be shown that

$$C_m = \frac{C_d}{(1+\tan^2\delta_m)} \quad (1)$$

$$\tan\delta_m = \omega C_d R_s + \tan\delta_d \quad (2)$$

where C_m and $\tan\delta_m$ are the measured capacitance and loss tangent of the parallel plate capacitor. C_d and $\tan\delta_d$ are the true capacitance and loss tangent of the dielectric film. These two equations enable us to determine the true capacitance and loss tangent of the dielectric film at higher frequencies [20]. For $Ba_{0.5}Sr_{0.5}TiO_3$ film on $Pt/Ti/SiO_2/Si$ substrate with Au/Cr top electrodes the R_s can be estimated to be about 1.1 Ω. The value of series resistance R_s was experimentally determined by measuring two capacitors of different sizes assuming that R_s and $\tan\delta_d$ are independent of frequency at mid frequency range. This modest value is compatible with most of the reported values for electrode and contact resistance [21]. Assuming $R_s = 1.1$ Ω and using the Equations 1 and 2, the effect of electrodes and contacts on the relative permittivity and loss tangent were corrected and given in Fig. 7. The relative permittivity and loss tangent after correcting for the electrode resistance is almost frequency independent at higher frequencies. At lower frequency measurements, typically less than 1 MHz, the contribution from electrode resistance and contacts are negligible and the measured losses correspond to the true dielectric losses. The dielectric data up to 100 MHz seems to agree quite well with our equivalent circuit model and subsequent corrections. Further investigations and substantial effort must be made to improve the dielectric measurements at frequencies higher than 100 MHz.

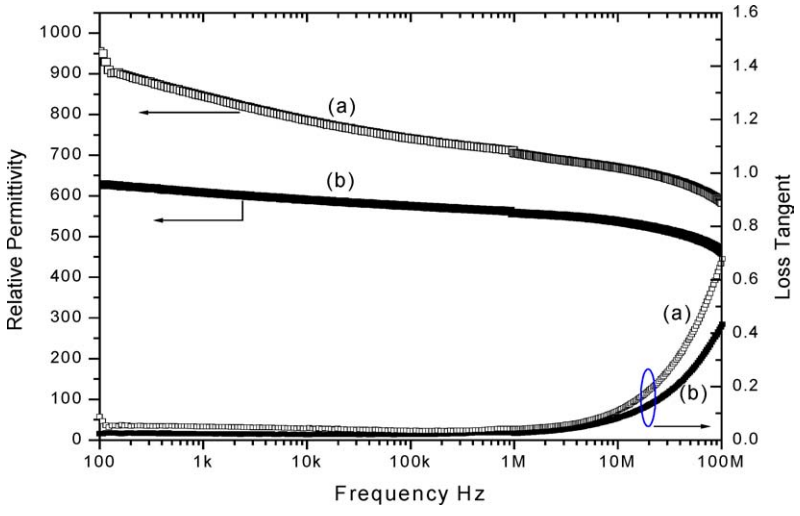

Figure 5 Relative permittivity and loss tangent as a function of frequency for $Ba_xSr_{1-x}TiO_3$ thin films: (a) $Ba_{0.7}Sr_{0.3}TiO_3$ and (b) $Ba_{0.5}Sr_{0.5}TiO_3$.

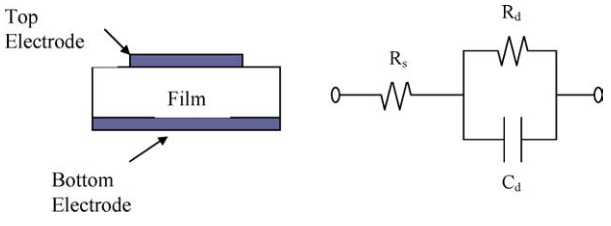

Figure 6 Equivalent circuit for the parallel plate capacitor with the electrode and contact resistance R_s, capacitance of the film C_d and true resistance of the film R_d.

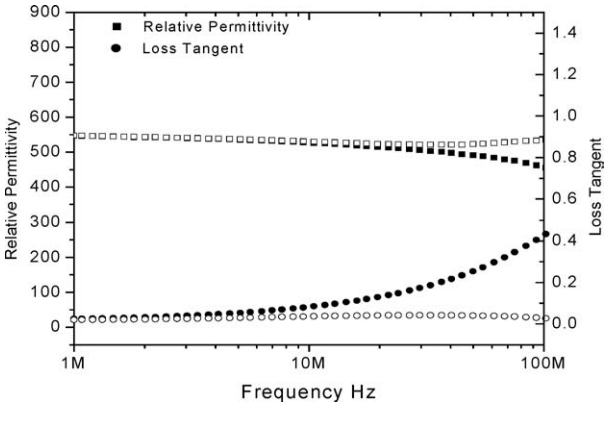

Figure 7 Measured and corrected relative permittivity and loss tangent for $Ba_{0.5}Sr_{0.5}TiO_3$ thin film. Solid symbols denote the measured data. The open symbols denote the true relative permittivity and loss tangent for the thin film after correcting for electrode and contact effects.

4. Conclusions

The use of modified sol-gel technique for thin film fabrication has improved the grain growth and crystallinity of $Ba_xSr_{1-x}TiO_3$ thin films. Glancing incidence X-ray diffraction patterns of the films showed that these BST films possess crystalline perovskite phase with all the characteristic peaks. The Curie temperature of $Ba_{0.7}Sr_{0.3}TiO_3$ thin film is around room temperature ($\sim$20°C) and hence $Ba_{0.7}Sr_{0.3}TiO_3$ composition possesses larger relative permittivity and dielectric tunability compared to that of other compositions. The dielectric dispersion with frequency is negligible in the paraelectric compositions, especially in $Ba_{0.5}Sr_{0.5}TiO_3$ thin films. Only two compositions, namely $Ba_{0.7}Sr_{0.3}TiO_3$ and $Ba_{0.8}Sr_{0.2}TiO_3$ showed P-E hysteresis loops at room temperature indicating the presence of ferroelectricity. These compositions showed significant dielectric dispersion and lower tunability at higher frequencies. The dielectric tunability of $Ba_{0.5}Sr_{0.5}TiO_3$ film is about 35.6% and for $Ba_{0.6}Sr_{0.4}TiO_3$ film is about 36.1% at 100 kHz. However the tunability of $Ba_{0.5}Sr_{0.5}TiO_3$ thin films has decreased from about 36 to 32% with the increase of frequency from 100 kHz to 100 MHz. As the frequency increases, especially above 10 MHz, relative permittivity decreases while the loss tangent increases. This behaviour originates from the contact resistance and finite sheet resistance of both the bottom and top electrodes. These effects from electrode resistance can be modelled using an equivalent circuit and can be corrected. After removing the parasitic resistance due to metallization, the relative permittivity and loss tangent of thin film is almost frequency independent up to 100 MHz.

Acknowledgments

This work was supported by the Centre for smart Materials of the Hong Kong Polytechnic University.

References

1. J. F. SCOTT, *Integr. Ferroelectrics* **20** (1–4) (1998) 15.
2. R. E. JONES, P. ZURCHER, P. CHU, D. J. TAYLOR, Y. T. LIJI, B. JIANG, P. D. MANIAR and S. J. GILLESPIE, *Microelectr. Engng.* **29** (1995) 3.
3. D. DAMJANOVIC, *Rep.Prog. Phys.* **61** (1998) 1267.
4. D. O'NEILL, G. CATALAN, F. PORRAS, R. M. BOWMAN and J. M. GREGG, *J. Mater. Sci. Mater. Electron.* **9** (1998) 199.
5. T. Y. TSENG, *Ferroelectrics* **232** (1999) 1.
6. J. S. HORWITZ, W. CHANG, W. KIM, S. B. QADRI, J. M. POND, S. W. KIRCHOEFER and D. B. CHERISEY, *J. Electroceram.* **4**(2/3) (2000) 357.
7. V. K. VARADAN, K. A. JOSE and V. V. VARADAN, *Smart Mater. Struct.* **8** (1999) 238.
8. D. DIMOS and C. H. MULLER, *Annu. Rev. Mater. Sci.* **28** (1998) 397.
9. S. U. ADIKARY, A. L. DING and H. L. W. CHAN, *Appl. Phys.* A **75** (2002) 597.

10. F. M. PONTES, E. LONGO, E. R. LEITE and J. A. VARELA, *Thin Solid Films* **386** (2001) 91.
11. S. U. ADIKARY and H. L. W. CHAN, *Ferroelectrics* **271** (2002) 277.
12. P. C. JOSHI, S. RAMANATHAN, S. B. DESU and S. STOWELL, *Phys. Stat. Sol.* (a) **161** (1997) 361.
13. A. OUTZOURHIT, J. U. TREFNY, T. KITO, B. YARAR, A. NAZIRIPOUR and A. HERMANN, *Thin Solid Films* **259** (1995) 218.
14. A. TOMBAK, J. P. MARIA, F. AYGUAVIVES, Z. JIN, G. T. STAUF, A. I. KINGON and A. MORTAZAWI, *IEEE Micowave Wirel. Comp. Lett.* **12** (2002) 3.
15. M. P. McNEAL, S. J. JANG and R. E. NEWNHAM, *J. Appl. Phys.* **83** (1998) 3288.
16. E. K. AKDOGAN, J. BELLOTTI and A. SAFARI, in Proceedings of the IEEE International Symposium on Applied Ferroelectrics (2000) Vol. 1, p. 191.
17. P. K. SINGH, S. COCHRANE, W. T. LIU, K. CHEN, D. B. KNORR, J. M. BORREGO and E. J. RYMASZEWSKI, *Appl. Phys. Lett.* **66** (1995) 3683.
18. J. D. BANIECKI, R. B. LAIBOWITZ, T. M. SHAW, P. R. DUNCOMBE, D. A. NEUMAYER, D. E. KOTECKI, H. SHEN and Q. Y. MA, *ibid.* **72** (1998) 498.
19. F. AYGUAVIVES, Z. JIN, A. TOMBAK, J. P. MARIA, A. MORTAZAWI and A. I. KINGON, *Integr. Ferroelectrics* **39** (2001) 393.
20. A. MANSINGH and M. SAYER, in Proceedings of the Ninth IEEE International Symposium on Applications of Ferroelectrics (ISAF '94), (University Park, PA, USA, 1995) p. 663.
21. D. C. DUBE, J. BABOROWSKI, P. MURALT and N. SETTER, *Appl. Phys. Lett.* **74** (1999) 3546.

Received 11 July 2003
and accepted 3 June 2004